Original Article

Comparison of ROS1-rearrangement detection methods in a cohort of surgically resected non-small cell lung carcinomas

Viktoria Thurfjell[1#], Patrick Micke[1#], Hui Yu[1], Rosemarie Krupar[2,3], Maria A. Svensson[4], Hans Brunnström[5], Kristina Lamberg[6], Lotte N. J. Moens[1,7], Carina Strell[1], Miklos Gulyas[1], Gisela Helenius[8], Akihiko Yoshida[9], Torsten Goldmann[2,10*], Johanna Sofia Margareta Mattsson[1*^]

[1]Department of Immunology, Genetics and Pathology, Uppsala University, Uppsala, Sweden; [2]Division of Pathology, Research Center Borstel, Leibniz Lung Center, Borstel, Germany; [3]Institute of Pathology, University Hospital Schleswig-Holstein, Campus Lübeck, Lübeck, Germany; [4]Clinical Research Center, Faculty of Medicine and Health, Örebro University, Örebro, Sweden; [5]Division of Pathology, Lund University and Laboratory Medicine Region Skåne, Lund, Sweden; [6]Department of Pulmonary and Allergic Diseases, Uppsala University Hospital, Uppsala, Sweden; [7]Clinical Genomics Uppsala, Science for Life Laboratory, Uppsala, Sweden; [8]Department of Laboratory Medicine, Faculty of Medicine and Health, Örebro University, Örebro, Sweden; [9]Department of Diagnostic Pathology, National Cancer Center Hospital, Tokyo, Japan; [10]Airway Research Center North (ARCN), Member of the German Center for Lung Research (DZL), Großhansdorf, Germany

Contributions: (I) Conception and design: P Micke, JSM Mattsson, V Thurfjell, T Goldmann; (II) Administrative support: P Micke, M Gulyas; (III) Provision of study materials or patients: P Micke, H Brunnström, K Lamberg, M Gulyas; (IV) Collection and assembly of data: T Goldmann, R Krupar, V Thurfjell, JSM Mattsson, H Brunnström, G Helenius, A Yoshida, MA Svensson, H Yu, C Strell; (V) Data analysis and interpretation: T Goldmann, R Krupar, MA Svensson, LNJ Moens, V Thurfjell, JSM Mattsson, P Micke, A Yoshida, H Yu, C Strell; (VI) Manuscript writing: All authors; (VII) Final approval of manuscript: All authors.

[#]These authors contributed equally to this work.

[*]These authors contributed equally for the senior authorship.

Correspondence to: Johanna Sofia Margareta Mattsson, PhD. Department of Immunology, Genetics and Pathology, Uppsala University, 75185 Uppsala, Sweden. Email: johanna.mattsson@igp.uu.se.

Background: Patients with non-small cell lung cancer (NSCLC) harboring a ROS proto-oncogene 1 (ROS1)-rearrangement respond to treatment with ROS1 inhibitors. To distinguish these rare cases, screening with immunohistochemistry (IHC) for ROS1 protein expression has been suggested. However, the reliability of such an assay and the comparability of the antibody clones has been debated. Therefore we evaluated the diagnostic performance of current detection strategies for ROS1-rearrangement in two NSCLC-patient cohorts.

Methods: Resected tissue samples, retrospectively collected from consecutive NSCLC-patients surgically treated at Uppsala University Hospital were incorporated into tissue microarrays [all n=676, adenocarcinomas (AC) n=401, squamous cell carcinomas (SCC) n=213, other NSCLC n=62]. ROS1-rearrangements were detected using fluorescence in situ hybridization (FISH) (Abbott Molecular; ZytoVision). In parallel, ROS1 protein expression was detected using IHC with three antibody clones (D4D6, SP384, EPMGHR2) and accuracy, sensitivity, and specificity were determined. Gene expression microarray data (Affymetrix) and RNA-sequencing data were available for a subset of patients. NanoString analyses were performed for samples with positive or ambiguous results (n=21).

Results: Using FISH, 2/630 (0.3% all NSCLC; 0.5% non-squamous NSCLC) cases were positive for ROS1 fusion. Additionally, nine cases demonstrated ambiguous FISH results. Using IHC, ROS1 protein expression was detected in 24/665 (3.6% all NSCLC; 5.1% non-squamous NSCLC) cases with clone D4D6, in 18/639 (2.8% all NSCLC; 3.9% non-squamous NSCLC) cases with clone SP384, and in 1/593 (0.2% all NSCLC; 0.3% non-squamous NSCLC) case with clone EPMGHR2. Elevated RNA-levels were seen in 19/369 (5.1%) cases (Affymetrix and RNA-sequencing combined). The overlap of positive results between

^ ORCID: 0000-0002-5294-7808.

the assays was poor. Only one of the FISH-positive cases was positive with all antibodies and demonstrated high RNA-expression. This rearrangement was confirmed in the NanoString-assay and also in the RNA-sequencing data. Other cases with high protein/RNA-expression or ambiguous FISH were negative in the NanoString-assay.

Conclusions: The occurrence of ROS1 fusions is low in our cohorts. The IHC assays detected the fusions, but the accuracy varied depending on the clone. The presumably false-positive and uncertain FISH results questions this method for detection of ROS1-rearrangements. Thus, when IHC is used for screening, transcript-based assays are preferable for validation in clinical diagnostics.

Keywords: Crizotinib; ROS proto-oncogene 1 (ROS1); fusion gene detection; molecular pathology; targeted therapy

Submitted Jul 04, 2022. Accepted for publication Nov 06, 2022.
doi: 10.21037/tlcr-22-504
View this article at: https://dx.doi.org/10.21037/tlcr-22-504

Introduction

Targeted therapy is a cornerstone of lung cancer treatment, with high response rates in subsets of non-small cell lung cancer (NSCLC) patients harboring an activating genomic aberration in tyrosine kinase receptors (TKRs). However, aside from the prototypic molecular subset of EGFR mutations that is detected in 10–50% of patients (1,2), most TKR aberrations, including ALK, RET, NTRK, and ROS proto-oncogene 1 (ROS1) fusions, are rare (3). Incidences range from <1% to 13% (4-12). ROS1-rearrangements were discovered in 2007, and the incidence in NSCLC patients is reported to be 1–2% (8-11). ROS1, located on the 6q22 chromosome, encodes a TKR that is closely related to the tyrosine kinase insulin receptor family (13-16). In ROS1-rearrangements, a split at the 5' end of exon 32, 34, 35, or 36 causes the 3' end, which encodes the protein's kinase domain, to fuse with a new 5' partner, leading to constitutive activation of the ROS1 kinase. The most common ROS1 fusion partner is CD74; however, other fusion partners have been identified, such as EZR, TPM3, SDC4, and SCL34A2 (17,18).

Currently, two targeted drugs are approved by the USA Food and Drug Administration (FDA) for the treatment of patients with ROS1 fusion. The first is crizotinib, which was primarily developed for treating ALK-fusion-positive NSCLC patients. Due to the homology between ROS1 and ALK, crizotinib has demonstrated efficacy also in ROS1-fusion-positive patients, with response rates around 77.6% reported in a large meta-analysis (19). The second approved drug is the second-generation multikinase inhibitor entrectinib. It has shown an overall response rate of 67.1% for ROS1 fusion-positive patients, including patients with brain metastasis (20). These two drugs have also been approved by the European Medicines Agency (EMA), with the requirement of a validated assay for detection of ROS1 fusion before treatment (21,22). Therefore, the accurate detection of ROS1-positive NSCLC patients is of great importance.

Fluorescence in situ hybridization (FISH) has long been regarded as the gold standard technique for the detection of ROS1-rearrangements (17). Most commonly, a split (break apart) probe is used for diagnostic purposes. FISH can be used to identify fusions regardless of the fusion partner and is considered a sensitive and specific method. However, FISH is time-consuming, relatively expensive, requires training, and needs special equipment (17).

Since fusions of ROS1 are often associated with high expression of the corresponding fusion protein (17,23), the use of immunohistochemistry (IHC) as a diagnostic screening tool has been suggested. In the case of positive protein expression, which is indicative of the presence of a fusion transcript, FISH or a molecular analysis is required for confirmation (24,25). To date, there are two commonly used commercially available ROS1 antibody clones: clone D4D6 from Cell Signaling and clone SP384 from Ventana Medical Systems. The latter is also part of the first *in vitro* diagnostic (IVD)/US class I ROS1 IHC assay. Recently, another commercially available clone, EPMGHR2 from Zytomed Systems, was introduced. Naturally, the use of different clones and assay protocols results in different staining patterns. Furthermore, evaluation is subjective as it is based on the pathologist's interpretation, and the

choice of the cut-off value used to define a positive result is crucial for any screening approach. Therefore, the aim of this study was to evaluate the diagnostic performance of current detection strategies for ROS1-rearrangement in two large Swedish NSCLC patient cohorts. We present the following article in accordance with the STARD reporting checklist (available at https://tlcr.amegroups.com/article/view/10.21037/tlcr-22-504/rc).

Methods

Study population and clinical characteristics

The study population consisted of two large retrospective NSCLC patient cohorts, a total of 676 patients consecutively surgically resected at Uppsala University Hospital between 1995 and 2010 (Tables S1,S2).

The first cohort (Uppsala I) included 358 patients operated on between 1995 and 2005. Formalin-fixed paraffin embedded (FFPE) tissue blocks were available for 352 of these patients, and cores from these blocks were included in a tissue microarray (TMA) as previously described (26,27). Fresh frozen tissue was available for 187 of these patients, and RNA was extracted from these tissue blocks and used in an Affymetrix gene expression microarray analysis. Fresh frozen tissue and Affymetrix gene expression microarray data were also available for six additional patients; however, due to a lack of FFPE material for these patients, they were not included in the study population.

The second cohort (Uppsala II) included 324 NSCLC patients operated on between 2006 and 2010 (28-30). FFPE tissue blocks were available from all of these patients, and cores from these tissue blocks were included in a TMA. Fresh frozen tissue was available for 182 of these patients, and RNA was extracted from these tissue blocks and used for Illumina RNA-sequencing analysis (31).

Information regarding the patients' clinical parameters (i.e., age at diagnosis, smoking history, gender, tumor histology, tumor stage, performance status according to WHO) and overall survival time was obtained from the records of the population-based Regional Lung Cancer Register (Tables S1,S2). The study was conducted in accordance with the Swedish Biobank legislation, performed in adherence with the Declaration of Helsinki (as revised in 2013), and approved by the Uppsala Regional Ethical Review Board (Uppsala I: 2006/325; Uppsala II: 2012/532) and individual consent for this retrospective analysis was waived.

Tissue microarray (TMA) construction

TMAs were constructed from FFPE tissue blocks. All tissue specimens were reviewed by pathologists [Uppsala I (PM) and Uppsala II (HB, PM)], and representative tumor areas were identified and encircled on hematoxylin-eosin-stained slides. Tissue cores were punched from the encircled areas using a manual tissue arrayer (MTA-1, Beecher Instruments, Sun Prairie, CA, USA). All tumors were included in duplicate (2 × 1 mm tissue cores) (26-29). Four micrometer-thick sections were taken from the blocks, mounted on adhesive slides (SuperFrost Ultra Plus, Thermo Fisher Scientific, Fermont, CA, USA), and used in the subsequent analyses.

Fluorescence in situ hybridization (FISH)

ROS1-rearrangement status was assessed by performing FISH on tissue of both NSCLC cohorts (Uppsala I and Uppsala II) that were represented by two sets of TMAs (each TMA included two different tissue cores from each tumor). In the first round, the Vysis 6q22 ROS1 Break Apart FISH Probe Kit (RUO) (08N29-020) (Abbott Molecular, Des Plaines, IL, USA) was used and analyzed at the Örebro Laboratory. Due to the detachment of some cores during the process, or because some cores did not include sufficient tumor cells, we repeated the FISH hybridization. Since the hybridization this time was performed in the Borstel Laboratory, a locally established FISH assay was used (ZytoMation ROS1 Dual Color Break Apart FISH Probe (Z-2298), ZytoVision GmbH, Bremerhaven, Germany).

The Vysis 6q22 ROS1 Break Apart FISH Probe Kit (RUO) (08N29-020) was used with the Vysis Paraffin Pretreatment IV & Post-Hybridization Wash Buffer Kit (CE) (01N31-005) according to the manufacturer's instructions. The TMA slides were baked at 60 ℃ for 1 h, followed by deparaffinization and rehydration. Pretreatment was performed at 80 ℃ for 35 min, followed by protease treatment at 37 ℃ for 40 min. The slides were then dehydrated, and denaturation of DNA was performed at 73 ℃ for 3 min, followed by probe hybridization at 37 ℃ overnight. Post-hybridization wash was performed at 75 ℃ for 3 min, and the slides were then mounted using ProLong® Gold Antifade Mountant with 4',6-diamidino-2-phenylindole (DAPI) (Thermo Fisher Scientific, Waltham, MA, USA). Analysis of the slides was performed under an oil immersion objective (×60 to ×100) using an Olympus

BX-61 fluorescence microscope (Center Valley, PA, USA) equipped with filters to visualize the different wavelengths associated with the fluorescent probes.

The ZytoMation ROS1 Dual Color Break Apart FISH Probe (Z-2298) was used according to the manufacturer's instructions. The slides were baked at 60 ℃ for 1 h, followed by deparaffinization and rehydration. Pretreatment was performed for 15 min at 97 ℃ in citrate buffer (pH=6). Afterward, the slides were cooled down, rinsed in water, and dried at room temperature on a drying rack. Enzymatic digestion was performed with pepsin; each slide was covered with a coverslip and incubated for 3 min at 37 ℃ in a humid chamber. The slides were rinsed in 2× saline-sodium citrate (SSC) buffer for 5 min and then dehydrated by immersion in 70%, 80%, 90%, and 100% ethanol for 1 min each. The slides were dried at room temperature. Then, 15 µL of ROS 1 Dual Color Break Apart FISH Probe (Z-2298) was applied under a coverslip sealed with adhesive. The slides were incubated at 75 ℃ for 10 min and then at 37 ℃ in a humid chamber overnight. The slides were rinsed once with 1× wash buffer, twice for 5 min each with 1× wash buffer, and dehydrated in 70%, 80%, 90%, and 100% alcohol for 1 min each. The slides were dried at room temperature on a drying rack and then mounted using a drop of DAPI solution, and a coverslip was added with nail polish used for sealing. FISH was evaluated using a Nikon Eclipse 80i microscope (Nikon, Melville, NY, USA) equipped with a Plan Apo VC 60× lens using oil immersion. Images were taken using a Leica DFC 450c camera system and Fix Foto software (Joachim Koopmann Software, Germany).

Annotation for the FISH analysis

A tumor sample was considered positive for ROS1-rearrangement when at least 15% of 50 analyzed tumor cells displayed split probe signals or isolated 3' (green) signals (24). Only cases with at least 50 evaluable tumor cells were included in the analysis. The FISH evaluation was performed by two independent evaluators (TG and JSMM) without knowledge of the IHC results for ROS1 protein expression.

Immunohistochemical staining

Clone D4D6 from Cell Signaling

Immunohistochemical (IHC) staining was performed on TMA sections. The slides were baked for 45 min at 60 ℃, followed by deparaffinization and heat-induced epitope retrieval with targeted retrieval solution (high pH) (Dako, Santa Clara, CA, USA). The slides were then treated with 3% hydrogen peroxide for 20 min to block endogenous peroxidase activity, and then incubated with the primary monoclonal rabbit anti-ROS1 antibody (clone D4D6, 1:100, Cell Signaling Technology, Danvers, MA, USA) at 4 ℃ overnight. The staining reactivity was then detected using the EnVision-FLEX+ (Dako, Santa Clara, CA, USA).

Clone SP384 from Ventana Medical Systems

The TMA sections were baked for 45 min at 60 ℃. Antigen retrieval was performed using Ventana's CC1 buffer at 95 ℃ for 36 min. This was followed by incubation with the primary monoclonal rabbit anti-ROS1 antibody (clone SP384, RTU, Ventana Medical Systems, Tucson, AZ, USA) at 32 ℃ for 20 min at the BenchMark Ultra instrument (Ventana Medical Systems Inc.) in combination with the UltraView DAB IHC Detection kit, according to the manufacturer's instructions.

Clone EPMGHR2 from Zytomed Systems

The TMA sections were baked for 45 min at 60 ℃. Following baking, deparaffinization, rehydration, and heat-induced epitope retrieval (pH 9) was performed at the PT Link Module (Dako, Santa Clara, CA, USA). The slides were then stained according to the EnvisonFlex+ Rabbit protocol, high pH (Dako, Santa Clara, CA, USA), using the primary rabbit anti-ROS1 monoclonal antibody (clone EPMGHR2, 1:75, Zytomed Systems, Berlin, Germany) at ambient temperature for 30 min in a Dako Autostainer Link48 (Dako, Santa Clara, CA, USA).

Scanning and viewing

Slides stained with clone D4D6 (Cell Signaling) and clone SP384 (Ventana Medical Systems) were scanned at 20× magnification using an Aperio ScanScope XT (Aperio Technologies Inc., Vista, CA, USA) whole slide scanner to obtain high-resolution digital images. The images were viewed in the freely available ImageScope software (Aperio Technologies Inc., Vista, CA, USA).

Slides stained with clone EPMGHR2 (Zytomed Systems) were scanned at 20× magnification using a NanoZoomer S60 whole slide scanner (Hamamatsu Photonics K.K., Japan) to obtain high-resolution digital images. The images were viewed using the freely available NDP.view2 software (Hamamatsu Photonics K.K., Japan).

Annotation and cut-off values for the immunohistochemical staining

Protein expression was manually and independently annotated by two observers (VT and JSMM). The staining intensity for the three antibodies was graded using a four-point scale: negative [0], weak [1], moderate [2], and strong [3]. Only the strongest staining in the sample was taken into account. The fraction of stained tumor cells was evaluated as follows: 0% stained cells [0], 1–10% [1], 11–20% [2], 21–30% [3], 31–40% [4], 41–50% [5], 51–60% [6], 61–70% [7], 71–80% [8], 81–90% [9], and 91–100% [10]. The staining intensity of the strongest staining in the sample and fraction of stained cells were multiplied to obtain an overall score that ranged from 0 to 30. The samples were dichotomized in negative (score 0–12) or positive cases (score 14–30), that is, cases that showed moderate staining in at least 61% of the tumor cells or strong staining in at least 41% of the tumor cells were regarded as positive. Nonspecific staining in macrophages, giant cells, and type II pneumocytes was disregarded (17). When clone EPMGHR2 was used, several cores showed artifactual border staining, which was disregarded.

Gene expression analysis

For a subset of patients, gene expression data were available. RNA from fresh frozen tumor tissue from 187 of the Uppsala I cohort patients had previously been subjected to gene expression microarray analysis on the Affymetrix HG U133 Plus 2.0 arrays (54675 probe sets, Affymetrix, Santa Clara, CA, USA), as previously described (32,33). This Uppsala I microarray dataset is available in the Gene Expression Omnibus (GEO) data repository (GSE37745). Two ROS1 probe sets (207569_at; 244363_at) were present in the Affymetrix U133 Plus 2.0 chip set. The mean of all samples, plus two standard deviations, was defined as the cut-off, and the samples were dichotomized into high- and low- expression groups at a cut-off of 7.0.

RNA from fresh frozen tissue from 182 of the Uppsala II cohort patients had previously been subjected to RNA-sequencing (RNAseq), as previously described (31). Briefly, the Illumina TruSeq RNA Sample Prep Kit v2 with polyA selection was used to prepare the RNA samples for sequencing. Multiplex sequencing was performed with five samples per lane on Illumina HiSeq2500 instruments (Illumina, San Diego, USA), using the standard Illumina RNAseq protocol with a read length of 2×100 bases. The raw data has been uploaded, together with clinical information, to the GEO with accession number GSE81089 (http://www.ncbi.nlm.nih.gov/geo/). The mean of all samples, plus two standard deviations, was defined as the cut-off based on fragments per kilobase of transcript per million mapped reads (FPKM)-values. The samples were divided into groups with high- and low- expression values at the cut-off of 62.6.

NanoString fusion analysis

NanoString fusion analysis was performed when a sample showed a clear or possible positive FISH results, elevated protein expression in the IHC assay, or elevated RNA (n=21) (*Table 1*).

FFPE tissue sections (10 µm thick) were used for total RNA extraction using the RNeasy® FFPE kit (Qiagen, Hilden, Germany). This was followed by assessment of RNA quantity and quality (DV200) using an RNA Screen Tape on a 4200 TapeStation system (Agilent, Santa Clara, CA, USA). A custom-designed fusion gene assay, based on Lira *et al.* (34), was used to perform the NanoString digital counting. The probe sets were designed by NanoString Technologies (Seattle, WA, USA) and synthesized by Integrated DNA Technologies (Leuven, Belgium). Total RNA (250 ng of FFPE-derived RNA, and 100 ng of Horizon Discovery RNA fusion reference standard) was hybridized to a multiplexed mixture of reporter and capture probes complementary to the target sequences. Hybridization, clean-up, imaging and counting were performed using an nCounter FLEX Analysis System (NanoString Technologies), following the the manufacturer's instructions. Fusion prediction was made based on both the specific fusion probe expression and 3'/5' expression ratio, according to Lira *et al.* (34) (Table S3).

Detection of fusion gene transcripts in the RNAseq data set

The RNAseq data of 182 patients from the Uppsala II cohort were analyzed using the STAR-Fusion gene detection method (version STAR-2.7.8a) (35) to detect gene fusions based on pair-end reads. For the analysis, default parameters were used as well as the reference database GRCh38_gencode_v37_CTAT_lib_Mar012021.

Statistical analysis

The sensitivity, specificity, and accuracy of the ROS1 IHC

Table 1 Results of all cases with ROS proto-oncogene 1 (ROS1) positivity in at least one of the assays. Included in the table is also information about gender, histology, mucinous histology and smoking

ID	Gender	Histology	Mucinous histology	Smoking	FISH			IHC clone D4D6			IHC Clone SP384			IHC clone EPMGHR2			Affymetrix (AU)	RNAseq (FPKM)	NanoString
					Vysis	ZytoVision	Final result	Intensity	Quantity	Score	Intensity	Quantity	Score	Intensity	Quantity	Score			
12	Male	AC	No	Former	Neg	Neg	Neg	0	0	0	1	7	7	0	0	0	8.3551†		Neg
16	Female	AC	No	Former	n/a	Neg‡	Neg‡	1	4	4	1	6	6	0	0	0	5.7583		Neg
50	Female	AC	Yes	Never	Neg	n/a	Neg	2	10	20†	0	0	0	0	0	0			
70	Female	AC	No	Current	n/a	Neg	Neg	0	0	0	2	9	18†	2	4	8			
79	Female	AC	No	Former	Neg	Neg	Neg	0	0	0	1	1	1	0	0	0	7.8194†		
80	Female	AC	No	Current	Neg	Pos	Pos†	0	0	0	0	0	0	3	1	3	4.5198		Neg
111	Female	AC	No	Current	Neg	Neg‡	Neg‡	1	1	1	2	4	8	2	1	2	7.1644†		Neg
149	Male	SCC	No	Current	Neg	Neg‡	Neg‡	0	0	0	0	0	0	0	0	0	4.1058		Neg
156	Male	LC	No	Current	Neg	Neg‡	Neg‡	0	0	0	0	0	0	2	1	2	5.5008		Neg
160	Female	AC	No	Current	Neg	Neg	Neg	0	0	0	0	0	0	0	0	0	7.6278†		
162	Male	AC	No	Former	Neg	Neg	Neg	3	1	3	0	0	0	2	2	4	7.0598†		
193	Female	AC	No	Never	n/a	n/a	n/a	2	9	18†	3	4	12	999	999	999	5.5727		
209	Female	AC	No	Never	Neg‡	n/a	Neg‡	1	5	5	1	6	6	2	1	2	6.2952		Neg
210	Female	AC	No	Never	n/a	n/a	n/a	2	6	12	3	8	24†	111	111	111			
213	Female	AC	No	Current	n/a	n/a	n/a	3	5	15†	1	1	1	111	111	111	6.2885		
235	Female	AC	No	Former	Neg	Neg	Neg	1	1	1	1	4	4	0	0	0	7.5675†		
241	Male	AC	No	Former	n/a	Neg	Neg	0	0	0	2	2	4	0	0	0	7.1183†		
242	Female	AC	No	Never	n/a	Neg	Neg	2	1	2	3	6	18†	0	0	0			
244	Female	AC	No	Never	n/a	n/a	n/a	0	0	0	1	1	1	111	111	111	7.4559†		
249	Male	SCC	No	Former	n/a	n/a	n/a	3	10	30†	111	111	111	111	111	111	4.4718		Neg
302	Female	AC	No	Former	n/a	n/a	n/a	3	6	18†	3	10	30†	999	999	999	7.202†		Neg
306	Female	AC	No	Current	Neg	Neg	Neg	2	3	6	3	5	15†	0	0	0			
336	Female	LC	No	Current	Neg‡	n/a	Neg‡	999	999	999	999	999	999	999	999	999	4.6083		Neg
347	Male	AC	No	Former	Neg	Neg	Neg	1	9	9	2	7	14†	0	0	0	5.6127		
368	Male	SCC	No	Former	Neg	Neg	Neg	0	0	0	3	5	15†	0	0	0			

Table 1 (*continued*)

Table 1 (*continued*)

ID	Gender	Histology	Mucinous histology	Smoking	FISH			IHC clone D4D6			IHC Clone SP384			IHC clone EPMGHR2			Affymetrix (AU)	RNAseq (FPKM)	NanoString
					Vysis	ZytoVision	Final result	Intensity	Quantity	Score	Intensity	Quantity	Score	Intensity	Quantity	Score			
375	Female	LC	No	Current	Neg	Neg	Neg	0	0	0	2	3	6	0	0	0	7.5804†		
L419	Female	AC	No	Former	Neg	Neg	Neg	3	5	15†	3	10	30†	0	0	0			Neg
L471	Male	AdSq	No	Never	Neg	Neg	Neg	2	1	2	3	1	3	0	0	0		66.956†	
L493	Female	AC	No	Current	Neg‡	n/a	Neg‡	2	6	12	1	7	7	3§	3§	9§		33.004	Neg
L511	Female	AC	No	Never	Neg	Neg	Neg	3	6	18†	3	10	30†	1	1	1		162.029†	Neg
L542	Female	AC	No	Never	n/a	Neg	Neg	2	8	16†	1	1	1	2	1	2			
L543	Male	AC	Yes	Current	n/a	Neg	Neg	2	9	18†	0	0	0	2	1	2		9.98	
L567	Female	AC	No	Never	Pos	Pos§	Pos†	2	9	18†	2§	8§	16†§	3§	8§	24†§		161.472†	Pos (SLC34A2-ROS1, S13del2046:R32)†
L611	Male	LCNEC	No	Current	n/a	Neg	Neg	2	9	18†	1	4	4	1	1	1			
L621	Female	AC	No	Former	Neg	Neg	Neg	2	4	8	2	4	8	0	0	0		88.150†	
L623	Female	AC	Yes	Current	Neg	Neg	Neg	2	8	16†	1	9	9	2	6	12			
L662	Male	AC	No	Former	Neg	Neg	Neg	2	2	4	2	3	6	2	1	2		71.476†	
L663	Female	AC	No	Current	Neg	n/a	Neg	3	10	30†	3	5	15†	2	1	2		5.075	Neg
L679	Female	AC	No	Never	n/a	Neg	Neg	2	9	18†	2	10	20†	2	1	2			
L689	Male	AC	Yes	Never	Neg	n/a	Neg	3	1	3	111	111	111	111	111	111		75.426†	
L692	Female	AC	No	Current	Neg	Neg	Neg	2	2	4	2	7	14†	0	0	0			
L695	Female	AC	Yes	Never	Neg	Neg	Neg	2	7	14†	2	8	16†	2	4	8		41.732	n/a
L724	Female	LC	No	Current	Neg	Neg‡	Neg‡	0	0	0	0	0	0	0	0	0		1.759	Neg
L732	Male	AC	Yes	Former	Neg	Neg	Neg	2	8	16†	0	0	0	0	0	0			
L743	Female	AC	No	Never	Neg	Neg	Neg	2	9	18†	2	10	20†	1	2	2			
L757	Male	AC	No	Former	Neg	Neg	Neg	2	10	20†	2	10	20†	0	0	0			
L761	Female	AC	Yes	Former	Neg	Neg	Neg	2	10	20†	111	111	111	111	111	111			
L769	Male	AC	No	Former	Neg	Neg	Neg	2	8	16†	1	1	1	1	1	1			
L814	Male	AC	No	Former	Neg	Neg	Neg	1	8	8	2	8	16†	0	0	0		33.9532	
L823	Female	AC	Yes	Current	Neg	n/a	Neg	3	8	24†	0	0	0	111	111	111			Neg

Table 1 (*continued*)

Table 1 (*continued*)

ID	Gender	Histology	Mucinous histology	Smoking	FISH			IHC clone D4D6		IHC Clone SP384		IHC clone EPMGHR2			Affymetrix (AU)	RNAseq (FPKM)	NanoString
					Vysis	ZytoVision	Final result	Intensity	Quantity	Score	Intensity	Quantity	Score	Intensity	Quantity	Score			
L828	Female	AC	Yes	Never	Neg	Neg	Neg	2	7	14[†]	2	4	8	2	1	2		39.1479	
L831	Female	AC	No	Current	Neg	Neg	Neg	2	8	16[†]	2	5	10	0	0	0		11.3418	
L832	Female	AC	No	Former	Neg	Neg	Neg	2	2	4	3	3	9	0	0	0		69.3393[†]	
L865	Female	AC	No	Current	Neg	n/a	Neg	3	10	30[†]	2	10	20[†]	2	1	2		28.557	Neg
L874	Female	AC	No	Current	Neg	Neg	Neg	3	2	6	2	4	8	3	4	12		91.2207[†]	Neg
L413 T1	Female	AC	No	Former	Neg[‡]	Neg	Neg[‡]	2	2	4	2	4	8	1	1	1		88.5403[†]	Neg

[†], sample defined as positive according to the cut-off; [‡], ambiguous FISH-result, but the sample was regarded as negative; [§], This protein expression annotation was performed on whole sections; 111, no tissue on TMA; 999, no cancer on TMA. FISH, fluorescence in situ hybridization; IHC, immunohistochemistry; RNAseq, RNA-sequencing; Neg and Pos, negative and positive; n/a, not applicable; AC, adenocarcinoma; SCC, squamous cell carcinoma; LC, large cell carcinoma; AdSq, adenosquamous carcinoma; LCNEC, large cell neuroendocrine carcinoma; TMA, tissue microarray.

and ROS1 FISH methods for predicting ROS1 status were calculated using the online MedCalc Software Ltd. Diagnostic test evaluation calculator (36). P values <0.05 were considered statistically significant.

Results

Patient characteristics

ROS1 status was assessed in a total of 676 NSCLC patients distributed over two independent cohorts, Uppsala I and Uppsala II. The patients' characteristics are shown in Tables S1,S2.

ROS1 status evaluated by FISH

It was possible to assess ROS1 status using FISH for 630 of the 676 (93.2%) cases represented on the TMAs (Tables S1,S2). In the non-assessable cases, the tissue cores were either missing on the TMAs, the tissue cores did not contain any tumor material, or the hybridization was insufficient for reliable evaluation. ROS1-rearrangement was identified in tumor samples from two (2/630=0.3%) patients, both were of adenocarcinoma histology (non-squamous NSCLC: 2/425=0.5%). In nine cases, the FISH result was considered to be ambiguous (*Table 1*). This was due to poor tissue quality or borderline results with clear split events in less than 15% of the tumor cells. However, since these cases did not fulfill the criteria for a positive FISH result, they were regarded as negative.

ROS1 status evaluated using immunohistochemistry (IHC)

ROS1 protein expression was evaluated using automated IHC with three different anti-ROS1 antibody clones: D4D6, SP384, and EPMGHR2. As the TMAs were sectioned between the staining procedures, some tumor material and tissue cores on the TMAs were lost over time. Therefore, different numbers of cases were available for evaluation with each antibody clone (Tables S1,S2).

Using clone D4D6, ROS1 status was evaluated in 665 (665/676=98.4%) cases. A positive result was defined as a sample with an immunohistochemical score of 14 or higher; that is, cases that showed moderate staining in at least 61% of the tumor cells or strong staining in at least 41% of the tumor cells were regarded as positive. With clone D4D6, positive results were found in 24 tumors (24/665=3.6%): 22 adenocarcinomas, one squamous cell cancer, and one

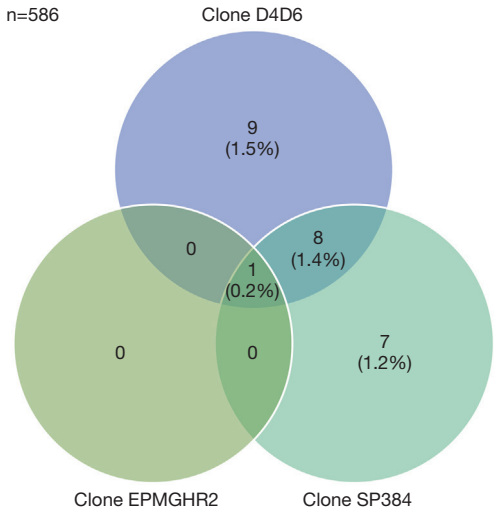

Figure 1 Venn diagram of the positive ROS proto-oncogene 1 (ROS1) staining based on the three antibody clones. The positive staining results of the anti-ROS1 antibody clones are compared. The cut-off for a positive result was set at a score 14, and cases with a lower score were regarded as negative.

large cell neuroendocrine carcinoma [non-squamous NSCLC: 23/454=5.1%; squamous cell carcinoma (SSC): 1/211=0.5%]. Of the ROS1- positive tumors, eight cases displayed strong homogeneous staining in 41% or more of the tumor cells, while the remaining 16 cases displayed moderate staining in at least 61% of the tumor cells.

Using clone SP384, ROS1 status was assessed in 639 patients (639/676=94.5%). Among these cases, 18 tumors (18/639=2.8%) returned positive results: 17 adenocarcinomas and one squamous cell cancer (non-squamous NSCLC: 17/432=3.9%; SCC: 1/207=0.5%). Of the ROS1-positive tumors, eight cases displayed strong homogeneous staining in more than 41% of the cells, while the remaining 10 tumors displayed moderate staining in more than 61% of the cells.

Using clone EPMGHR2, ROS1 status was assessed in 593/676 (87.7%) cases. One tumor (1/593=0.2%) was scored positive for ROS1, an adenocarcinoma (non-squamous NSCLC: 1/396=0.3%). The staining was strong and homogeneous in at least 71% of the tumor cells.

Immunohistochemical staining of whole tissue sections was performed for two cases with tissue missing from the TMA. One case returned a positive FISH result (L567), and the other showed an ambiguous FISH result and variable immunohistochemical staining (L493).

Comparison of the three anti-ROS1 antibody clones

Altogether, 586 (586/676=86.7%) cases were assessed with all three clones, and the immunohistochemical staining results were compared (*Figure 1*).

A total of 25 cases (4.3%) displayed positive staining with at least one antibody clone. Within this group, eight cases (1.4%) exhibited positive staining with two antibody clones (D4D6 and SP384), while only one case (0.2%; L567) displayed positive staining with all three clones. This was the only case considered to be positive for staining with clone EPMGHR2. However, it should be noted that the cases that were positively stained with one clone only showed focal staining with the other clones; however, this was regarded as negative based on the predefined cut-off value (*Table 1*). Five of the cases that displayed positive staining with only clone D4D6 were mucinous adenocarcinomas. It should be noted that tissues with mucinous histology may show positivity without ROS1-rearrangement (37). None of these five mucinous cases showed a ROS1-rearrangement with FISH.

Comparison of the FISH results and the IHC results

Concordance between the FISH and IHC results for detection of ROS1-rearrangements is of high importance, since IHC-based methods have been suggested as screening methods for this patient subset.

In our study, 626 tumors were evaluated with both FISH and IHC clone D4D6, 606 tumors with both FISH and IHC clone SP384, and 583 tumors with both FISH and IHC clone EPMGHR2 (*Figure 2*). Of the two FISH-positive tumors, one was found to stain positive with all IHC clones (L567) (*Figure 3*). This case showed moderate staining in more than 81% of the tumor cells with clone D4D6, moderate staining in more than 71% of the tumor cells with clone SP384, and strong staining in more than 71% of the tumor cells with clone EPMGHR2. The other FISH-positive case (L80) (*Figure 3*) was negative for staining with clones D4D6 and SP384; however, with clone EPMGHR2, strong staining was present in 1–10% of the tumor cells, although, this staining did not reach the cut-off value. Considering FISH as the reference method, the sensitivity of the D4D6 clone was 50% with a specificity of 97.1% and an accuracy of 97%, the sensitivity of the SP384 clone was 50% with a specificity of 97.3% and an accuracy of 97%, and the sensitivity of the EPMGHR2 clone was

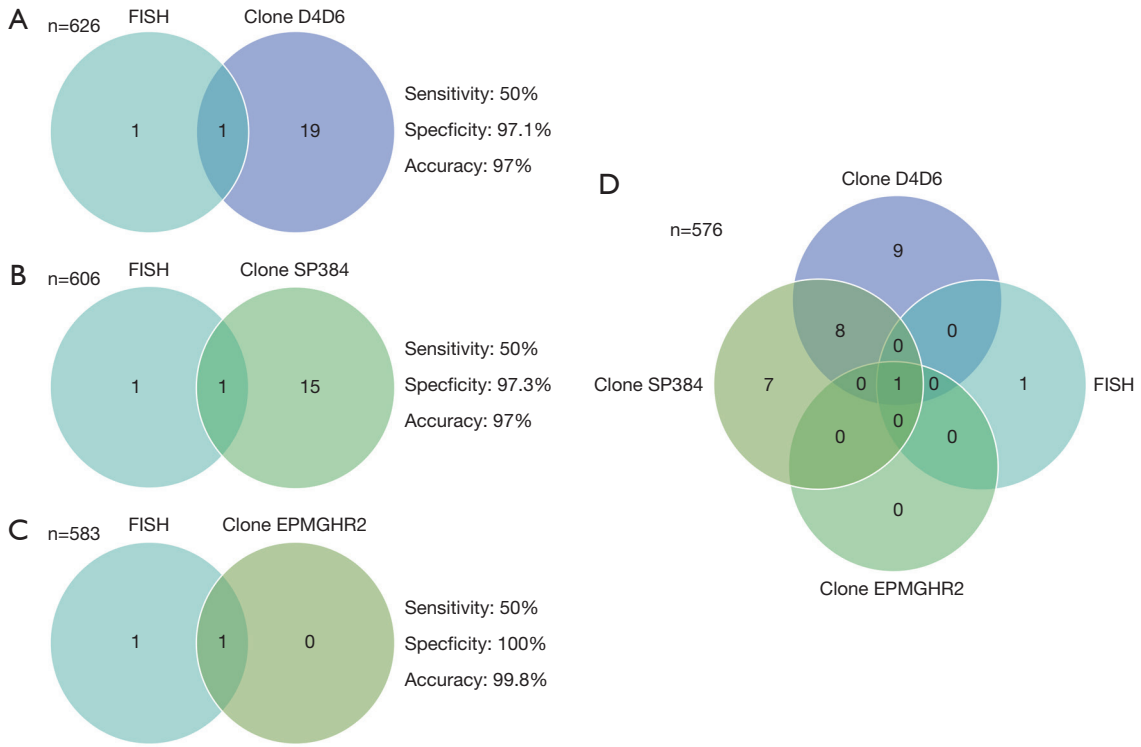

Figure 2 Venn diagram of the detection of ROS proto-oncogene 1 (ROS1) using different analytical methods. (A) Samples with positive fluorescence in situ hybridization (FISH) results were compared to samples that showed positive protein expression with the D4D6 immunohistochemistry (IHC) clone. Considering FISH as the reference method, the sensitivity of the D4D6 clone was 50%, with a specificity of 97.1% and an accuracy of 97%. (B) Samples with positive FISH results were compared to samples that showed positive protein expression with the SP384 IHC clone. Considering FISH as the reference method, the sensitivity of the SP384 clone was 50%, with a specificity of 97.3% and an accuracy of 97%. (C) Samples with positive FISH results were compared to samples that showed positive protein expression with the IHC clone EPMGHR2. Considering FISH as the reference method, the sensitivity of the EPMGHR2 clone was 50%, with a specificity of 100% and an accuracy of 99.8%. (D) Samples that stained positive with clones D4D6, SP384, and EPMGHR2 and had positive FISH results were compared.

50% with a specificity of 100% and an accuracy of 99.8% (*Figure 2*).

ROS1 gene expression

Fresh frozen tissue samples from 187 patients of the Uppsala I cohort (187/352=53.1%) were analyzed by Affymetrix gene expression microarray for ROS1 expression. When the cut-off of 7 AU was applied, 10 samples (10/187=5.3%) were considered to be positive; nine were of adenocarcinoma histology while one was a large cell carcinoma (non-squamous NSCLC: 10/125=8.0%). Among these 10 samples, only one sample returned a positive result with another assay (ID 302); in the IHC assay, it was stained with both clones D4D6 and SP384, while staining with clone EPMGHR2 was not evaluable (*Figure 4A*).

For 182 patients (182/324=56.2%) of the Uppsala II cohort, gene expression data based on RNAseq were available. Gene expression in normal lung tissue samples was in the range of 23–46 FPKM. While most of the tumor tissue samples displayed lower RNA-expression levels than those found in the normal lung tissue samples, nine samples (9/182=4.9%) had higher ROS1 RNA-levels and were considered positive according to our cut-off value. Of these nine samples, eight were of adenocarcinoma histology while one sample was of adenosquamous histology (non-squamous NSCLC: 9/121=7.4%). In particular, two cases expressed substantially higher FPKM values (L567 and L511) compared to the other tumor samples. One of these cases (L567) returned positive results in the FISH, NanoString,

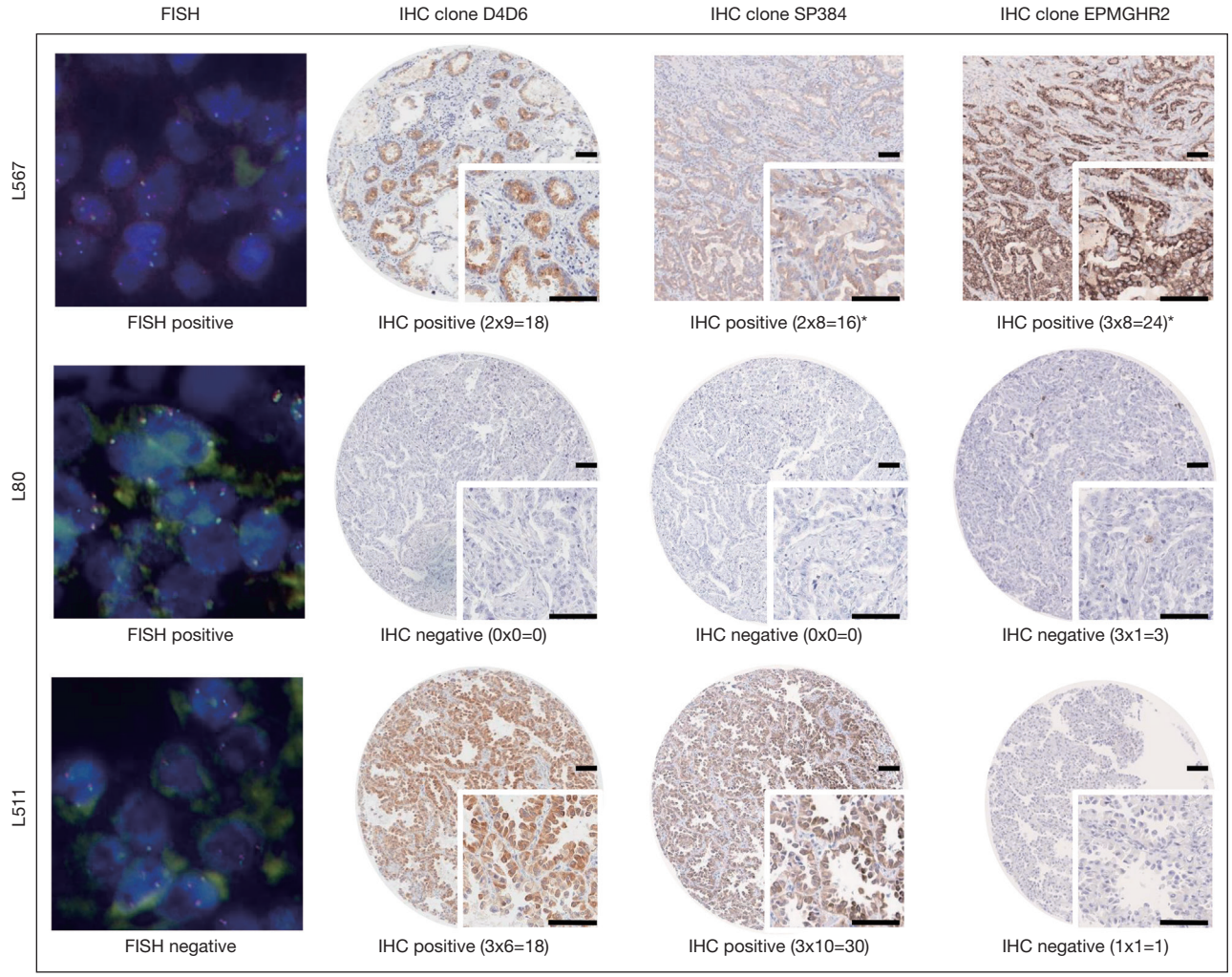

Figure 3 Visualization of the fluorescence in situ hybridization (FISH) and immunohistochemical (IHC) staining results. Case L567 showed a positive FISH result and positive staining with all three antibody clones. *Annotation of protein expression was performed on whole sections for clones SP384 and EPMGHR2. Case L80 showed a positive FISH result and negative staining with all three antibody clones. It should be noted that this case has previously shown immunoreactivity with other IHC stainings, and is therefore not regarded as a false ROS proto-oncogene 1 (ROS1) IHC negative case. Case L511 is included as an example of a case in which the FISH and clone EPMGHR2 results were negative, but staining with clones D4D6 and SP384 was positive. This case also displayed high gene expression levels based on RNA-sequencing. Scale bar represents 100 µm.

and IHC (with all three clones) assays, while the second case (L511) returned a positive result in only the IHC assay (with clones D4D6 and SP384) and did not show a molecular translocation (*Figure 4B*).

NanoString fusion analysis

The inconsistencies within and between the FISH and IHC assay results prompted us to conduct an orthogonal analysis on equivocal cases. For this, we selected cases that had at least one of the following attributes: (I) a positive FISH result, (II) an ambiguous FISH result, (III) elevated RNA-expression, or (IV) high protein expression detected with one of the clones. These cases (n=21) were subjected to a fusion gene assay based on the NanoString technique (*Table 1*).

Only one sample (L567) was confirmed as harboring a ROS1-rearrangement based on specific fusion probe expression (SLC34A2-ROS1, S13del2046:R32) and on the

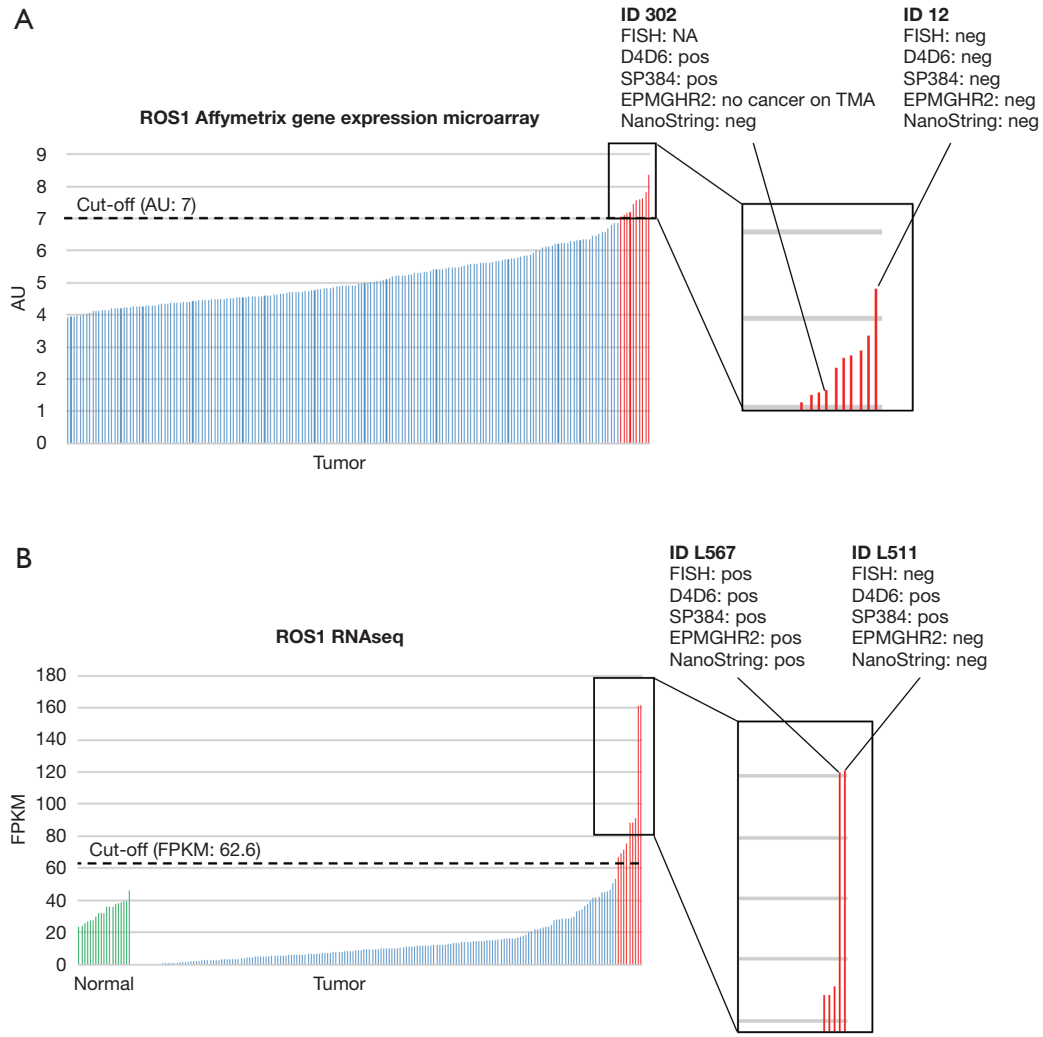

Figure 4 ROS proto-oncogene 1 (ROS1) gene expression detected using Affymetrix gene expression microarray and RNA-sequencing. (A) The histogram shows the mean values of the Affymetrix gene expression probe sets 207569_at and 244363_at from 187 non-small cell lung cancer (NSCLC) patients in the Uppsala I cohort. Gene expression signals are displayed as arbitrary units (AU). Samples determined to be positive according to our cut-off value are denoted in red. Samples with the highest gene expression levels are shown in the magnification. The results from the other assays are indicated for the case with the highest gene expression (ID 12) and for case ID 302, since this was the only case with a positive result in another assay of all the positive cases according to our gene expression cut-off value. (B) ROS1 RNA-expression from RNA-sequencing analysis of tumor tissue (n=182) and normal tissue (n=19) from 182 NSCLC patients included in the Uppsala II cohort. Normal expression is denoted in green, and tumor expression is denoted in blue. Samples determined to be positive according to our cut-off value are marked in red. The results from the other assays are indicated for the two cases with the highest RNA expression: L567 and L511. These two cases were the only ones that returned positive results in other assays. Gene expression signals are displayed as fragments per kilobase of transcript per million mapped reads (FPKM)-values. TMA, tissue microarray.

3'/5' expression imbalance. No other sample showed an indication of ROS1-rearrangement either by the specific fusion probes or 3'/5' expression imbalance (*Table 1*). Of the two FISH-positive cases, only one was considered to actually harbor a ROS1 fusion. With this knowledge, the overall frequency of ROS1-rearrangements was found to be even lower than that presumed using FISH, with a prevalence of 0.2% (1/630=0.2%) in these two large Swedish cohorts.

Detection of gene fusion transcripts in the RNAseq data set

The RNAseq data of 182 NSCLC patients were mapped to the human reference genome to identify discordantly mapping reads indicating potential somatic fusion genes using the STAR-Fusion gene detection method. This method also identified the FISH- and NanoString-positive case (L567) to contain the rearrangement SLC34A2-ROS1. In addition, an indication of fusion was found in sample L635. This fusion occurred between ROS1 and the long non-coding RNA (lncRNA) AL139042.1. In this case, ROS1 is the 5' partner, and not the 3' partner. For these reasons, this transcript most likely does not lead to the transcription of a functional protein. Sample L635 was negative with all three IHC antibody clones well as with FISH. In the FISH analysis, a pattern of isolated red signals was detected; however, this is not considered a criterion for rearrangement.

Discussion

In this study, we conducted one of the largest and most comprehensive characterizations of ROS1 status in NSCLC patients using three different detection strategies. We found that the incidence of ROS1 fusions in our study population was 0.2%, which is considerably lower than previously reported. As a screening tool for ROS1 protein expression, the IHC method was found to have a variable, possibly high false- positive rate. In addition, the reliability of the FISH method was found to be limited by technical and interpretational aspects.

In most previous studies, higher frequencies of ROS1-rearrangements have been reported. In perhaps the largest study of its kind (38), samples from 6,066 unselected Chinese NSCLC patients were analyzed using a real-time PCR approach, and 2.6% of the cases were determined to be harboring a ROS1 fusion. Also, Bergethon *et al.* (11) reported an incidence of 1.7% of ROS1 fusion-positive cases when they evaluated 1,073 unselected, mostly non-Asian NSCLC patients using FISH. In a Japanese study (8), a frequency of 0.9% was reported for rearranged cases detected among 1,476 NSCLC patients. Many smaller studies have reported the prevalence to be 2–4% in patients with both adenocarcinomas and squamous cell carcinomas, although squamous cell carcinomas rarely harbor ROS1 fusions (39-42). We found a considerably lower frequency of ROS1-rearrangements in our study (0.2%). A reason for this might be that ROS1-rearrangements are more frequent in advanced cancer patients (stages III–IV). This was suggested by the findings of a large meta-analysis conducted by Zhu *et al.* (43), which included 9,898 NSCLC patients from 18 studies. Whereas, our study primarily included patients with localized tumors who were surgically treated. Another reason for the low frequency in our cohort may be the relatively high proportion of squamous cell carcinomas (213/676=31.5%) as well as the low number of never-smokers in this cohort (10.2%).

Nevertheless, we believe that the low frequency found in our study population reflects the real incidence in Nordic countries and, more generally, in a European population. Similar findings were reported from an independent survey of a large advanced Swedish NSCLC patient cohort that used IHC and FISH for detection (44) and from an independent study of an Austrian NSCLC patient population (45). Low frequencies have also been reported for other gene rearrangements, such as ALK, RET, and NTRK (8,46,47).

The rearranged case in our study was detected by FISH and all three IHC antibody clones. However, the FISH also identified a second case as positive and several cases as ambiguous for ROS1-rearrangement. This second FISH-positive case (I) did not return a positive result with any of the IHC antibody clones, (II) displayed low ROS1 gene expression levels, and (III) did not show any imbalance in the NanoString analysis. Therefore, we regarded this case as a false-positive FISH result. This is problematic, because break-apart FISH has been the gold standard assay for the detection of ROS1-rearrangements, as the assay was used in early studies to determine the prevalence of ROS1 fusions as well as in the initial trials of crizotinib (11,48). It is worth noting that several limitations of this method have been described. The quality of FISH results depends on pre-analytical factors (e.g., fixation medium and fixation-time) as well as the storage of the FFPE-tissue blocks and the length of storage after cutting the sections. Also, the hybridization process can be crucial (24). Perhaps the most difficult step is the interpretation of the results, which can lead to both false-negative and false-positive results. The latter may be due to non-functional ROS1 fusions or to post-transcription and post-translation phenomena that inactivate the fusion product (24). Furthermore, aberrant probe hybridization has been reported (49,50). In addition, sectioning artifacts may lead to the occurrence of split signals as well as false single-red/single-green signals. Other limitations of the FISH approach include the lack of ability to identify the fusion partner (49,50). The existence of a false-positive and

several ambiguous FISH results in our study does not favor the use of FISH as a screening method or as a reference method for the detection of ROS1 fusion.

The effectiveness of IHC in the detection of ROS1 fusion products was also examined in this study. Some of the major advantages of using IHC to determine biomarker status are the ease, speed, and relatively low cost of performing and interpreting an IHC assay (51). These features are particularly important for the detection of low-prevalence biomarkers in NSCLC patients, such as RET, NTRK, ALK, and ROS1. However, there are no universally established immunostaining interpretative criteria for predicting gene rearrangement and no standard cut-off values for the definitive identification of ROS1 fusion products. The monoclonal antibodies D4D6 and EPMGHR2 are categorized as research-use-only (RUO) and used in assays with various protocols, visualization systems, and staining platforms, which leads to variation in staining and interpretation. The Ventana SP384 clone is part of the only approved *in vitro* diagnostic IHC assay for ROS1 and is used in conjunction with Ventana's staining instruments. They recommend setting the cut-off value as that at which there is moderate intensity in at least 30% of the total tumor cells (52,53). If we had applied this cut-off for the Ventana clone SP384 in our study, 16 additional cases (18+16=34, 34/639=5.3%) would have been considered positive. Thus, the false-positive rate would have been considerably higher.

In our study, the only confirmed ROS1 fusion case was detected by all three antibody clones; however, the accuracy varied depending on the clone used. The clone EPMGHR2 did not show any false-positives and thus provided a sensitivity and specificity of 100%. This optimal performance should still be interpreted with caution and confirmed in a cohort with more positive cases.

Nevertheless, both ROS1 protein and mRNA may be expressed in tumors that lack ROS1 fusions (24). False-positive IHC staining may also occur in ERBB2- and EGFR-mutated lung tumors (10,54-56), as well as in tumors with mucinous, lepidic, and/or acinar histologies (37,56,57). As a result, nonspecific ROS1 protein expression may be detected in ROS1-negative tumors, ranging from weak and patchy to strong and widespread (24,58). We also observed high RNA-expression levels in a number of cases that were not associated with ROS1 fusion.

Therefore, we recommend that the detection of ROS1 fusion by IHC is confirmed by either FISH or, preferably, at the transcript level. We used the NanoString system to detect the most common known fusion gene transcripts and to determine the ROS1 5' and 3' expression, where the 3'/5' expression ratio would generally indicate a ROS1 fusion. This assay has previously demonstrated strong concordance with the FISH and IHC assays, and a benefit of this approach is that it can be used to evaluate multiple fusion genes simultaneously (34,59).

It should be noted that transcript analysis is now often integrated in the NGS workflow, for example, in the TruSight Oncology 500 assay. When such comprehensive NGS assays are implemented for the routine analysis of NSCLC, screening approaches obviously become obsolete. This is in line with the latest guidelines of the ASCO (25,60), which recommend the use of a broad analytic strategy. In reality, in the near future, this scenario will only be achievable in larger cancer centers.

The major strengths with our study are the parallel and independent analysis with IHC and FISH on this real-world NSCLC patient population. There are also some limitations that should be considered when interpreting our results. First, we did not test all samples with the lung fusion panel from NanoString. Primarily, we focused on samples with positive IHC results and positive or ambiguous FISH results. As a result, we cannot be entirely sure that we captured all ROS1-rearranged cases in our cohorts. Second, the NanoString-specific probes only detect known fusion gene transcripts; thus, new fusions with unknown partners might have been missed. Therefore, the FISH-positive case (L80) that was negative in the NanoString analysis may be the case of a less common fusion. Third, since the ROS1 IHC and FISH assays were performed on TMAs, we potentially did not capture tumors with focal ROS1 expression. However, tumors with ROS1-rearrangements are most commonly diffusely positive, generally in a homogeneous fashion, with cytoplasmic staining ranging from weak to strong. Heterogeneity may be observed within a tumor; however, this is possibly a result of variable fixation in resected specimens (24). Indeed, TMAs with small tissue cores reflect the small sample size of biopsies most commonly used in routine diagnostics (61), and thus the clinical situation.

In conclusion, our findings indicate that the occurrence of ROS1 fusions is exceedingly low in resected NSCLC tissue samples. IHC assays can be used to detect these fusions with varying accuracy. Based on our experience, we do not favor the use of FISH as either a screening or reference method for the detection of ROS1-rearrangement in NSCLC. Thus, when IHC protocols are used for

screening, transcript-based assays are preferable for validation in clinical diagnostics.

Acknowledgments

We thank the Research and Development Unit of the Uppsala Pathology Department, Clinical Pathology at the Uppsala University Hospital, and Clinical Genomics Uppsala (Science for Life Laboratory) for technical assistance. We thank the Scribendi editor for editing and proofreading the manuscript.

Funding: This work was supported by the Swedish Cancer Society (CAN 2018/0716 to PM); Vetenskapsrådet (#2021-02693 to PM); Uppsala-Örebro Regional Research Council (Regionala forskningsrådet i Uppsala-Örebroregionen to PM); the Selanders Stiftelse, Uppsala Sweden (to JSMM); the Lions Cancer Foundation Uppsala, Sweden (to VT); and the Sjöberg Foundation, Sweden (to PM).

Footnote

Reporting Checklist: The authors have completed the STARD reporting checklist. Available at https://tlcr.amegroups.com/article/view/10.21037/tlcr-22-504/rc

Data Sharing Statement: Available at https://tlcr.amegroups.com/article/view/10.21037/tlcr-22-504/dss

Conflicts of Interest: All authors have completed the ICMJE uniform disclosure form (available at https://tlcr.amegroups.com/article/view/10.21037/tlcr-22-504/coif). VT reports support for study materials from the Lions Cancer Foundation, Uppsala, Sweden. PM reports support for the present manuscript from the Swedish Cancer Society, Vetenskapsrådet, Uppsala-Örebro Regional Research Council, and the Sjöberg Foundation. RK reports consulting fees from Aignostics GmbH. CS reports grants from the Swedish Cancer Society, Swedish Cancer Society Radiotherapy Fellowship, and Cancer- och Allergifonden Research. GH reports grants from Roche, honoraria from Bristol Meyer Squibb, payment for expert testimony from Astra Zeneca and Pfizer, and support for attending meetings and/or travel from Astra Zeneca. JSMM reports support for study materials from Selanders Stiftelse, Uppsala, Sweden, support for attending meetings from the Swedish Cancer Society, and receipt of materials from Zytomed Systems (anti-ROS1 mAb EPMGHR2). The other authors have no conflicts of interest to declare.

Ethical Statement: The authors are accountable for all aspects of the work in ensuring that questions related to the accuracy or integrity of any part of the work are appropriately investigated and resolved. The study was conducted in accordance with the Declaration of Helsinki (as revised in 2013). The study was approved by the Uppsala Regional Ethical Review Board (Uppsala I: 2006/325; Uppsala II: 2012/532) and individual consent for this retrospective analysis was waived.

References

1. Midha A, Dearden S, McCormack R. EGFR mutation incidence in non-small-cell lung cancer of adenocarcinoma histology: a systematic review and global map by ethnicity (mutMapII). Am J Cancer Res 2015;5:2892-911.
2. Nishii T, Yokose T, Miyagi Y, et al. Clinicopathological features and EGFR gene mutation status in elderly patients with resected non-small-cell lung cancer. BMC Cancer 2014;14:610.
3. Kohno T, Nakaoku T, Tsuta K, et al. Beyond ALK-RET, ROS1 and other oncogene fusions in lung cancer. Transl Lung Cancer Res 2015;4:156-64.
4. Soda M, Choi YL, Enomoto M, et al. Identification of the transforming EML4-ALK fusion gene in non-small-cell lung cancer. Nature 2007;448:561-6.
5. Shaw AT, Yeap BY, Mino-Kenudson M, et al. Clinical features and outcome of patients with non-small-cell lung cancer who harbor EML4-ALK. J Clin Oncol 2009;27:4247-53.
6. Horn L, Pao W. EML4-ALK: honing in on a new target in non-small-cell lung cancer. J Clin Oncol 2009;27:4232-5.
7. Guo Y, Ma J, Lyu X, et al. Non-small cell lung cancer with EML4-ALK translocation in Chinese male never-smokers is characterized with early-onset. BMC Cancer 2014;14:834.
8. Takeuchi K, Soda M, Togashi Y, et al. RET, ROS1 and ALK fusions in lung cancer. Nat Med 2012;18:378-81.

9. Rikova K, Guo A, Zeng Q, et al. Global survey of phosphotyrosine signaling identifies oncogenic kinases in lung cancer. Cell 2007;131:1190-203.
10. Li C, Fang R, Sun Y, et al. Spectrum of oncogenic driver mutations in lung adenocarcinomas from East Asian never smokers. PLoS One 2011;6:e28204.
11. Bergethon K, Shaw AT, Ou SH, et al. ROS1 rearrangements define a unique molecular class of lung cancers. J Clin Oncol 2012;30:863-70.
12. Vaishnavi A, Capelletti M, Le AT, et al. Oncogenic and drug-sensitive NTRK1 rearrangements in lung cancer. Nat Med 2013;19:1469-72.
13. Birchmeier C, O'Neill K, Riggs M, et al. Characterization of ROS1 cDNA from a human glioblastoma cell line. Proc Natl Acad Sci U S A 1990;87:4799-803.
14. Birchmeier C, Sharma S, Wigler M. Expression and rearrangement of the ROS1 gene in human glioblastoma cells. Proc Natl Acad Sci U S A 1987;84:9270-4.
15. Charest A, Lane K, McMahon K, et al. Fusion of FIG to the receptor tyrosine kinase ROS in a glioblastoma with an interstitial del(6)(q21q21). Genes Chromosomes Cancer 2003;37:58-71.
16. Nagarajan L, Louie E, Tsujimoto Y, et al. The human c-ros gene (ROS) is located at chromosome region 6q16---- 6q22. Proc Natl Acad Sci U S A 1986;83:6568-72.
17. Bubendorf L, Büttner R, Al-Dayel F, et al. Testing for ROS1 in non-small cell lung cancer: a review with recommendations. Virchows Arch 2016;469:489-503.
18. Davies KD, Doebele RC. Molecular pathways: ROS1 fusion proteins in cancer. Clin Cancer Res 2013;19:4040-5.
19. Vuong HG, Nguyen TQ, Nguyen HC, et al. Efficacy and Safety of Crizotinib in the Treatment of Advanced Non-Small-Cell Lung Cancer with ROS1 Rearrangement or MET Alteration: A Systematic Review and Meta-Analysis. Target Oncol 2020;15:589-98.
20. Dziadziuszko R, Krebs MG, De Braud F, et al. Updated Integrated Analysis of the Efficacy and Safety of Entrectinib in Locally Advanced or Metastatic ROS1 Fusion-Positive Non-Small-Cell Lung Cancer. J Clin Oncol 2021;39:1253-63.
21. xalkori-epar-product-information_en.pdf [Internet]. [cited 2022 Jun 22]. Available online: https://www.ema.europa.eu/en/documents/product-information/xalkori-epar-product-information_en.pdf
22. rozlytrek-epar-product-information_en.pdf [Internet]. [cited 2022 Jun 22]. Available online: https://www.ema.europa.eu/en/documents/product-information/rozlytrek-epar-product-information_en.pdf
23. Clavé S, Gimeno J, Muñoz-Mármol AM, et al. ROS1 copy number alterations are frequent in non-small cell lung cancer. Oncotarget 2016;7:8019-28.
24. Tsao MS, Hirsch FR, Yatabe Y, International Association for the Study of Lung Cancer. IASLC atlas of ALK and ROS1 testing in lung cancer. Aurora (Colorado): International Association for the Study of Lung Cancer; 2016.
25. Lindeman NI, Cagle PT, Aisner DL, et al. Updated Molecular Testing Guideline for the Selection of Lung Cancer Patients for Treatment With Targeted Tyrosine Kinase Inhibitors: Guideline From the College of American Pathologists, the International Association for the Study of Lung Cancer, and the Association for Molecular Pathology. J Thorac Oncol 2018;13:323-58.
26. Lohr M, Edlund K, Botling J, et al. The prognostic relevance of tumour-infiltrating plasma cells and immunoglobulin kappa C indicates an important role of the humoral immune response in non-small cell lung cancer. Cancer Lett 2013;333:222-8.
27. Edlund K, Lindskog C, Saito A, et al. CD99 is a novel prognostic stromal marker in non-small cell lung cancer. Int J Cancer 2012;131:2264-73.
28. Tran L, Mattsson JS, Nodin B, et al. Various Antibody Clones of Napsin A, Thyroid Transcription Factor 1, and p40 and Comparisons With Cytokeratin 5 and p63 in Histopathologic Diagnostics of Non-Small Cell Lung Carcinoma. Appl Immunohistochem Mol Morphol 2016;24:648-59.
29. Micke P, Mattsson JS, Djureinovic D, et al. The Impact of the Fourth Edition of the WHO Classification of Lung Tumours on Histological Classification of Resected Pulmonary NSCCs. J Thorac Oncol 2016;11:862-72.
30. La Fleur L, Falk-Sörqvist E, Smeds P, et al. Mutation patterns in a population-based non-small cell lung cancer cohort and prognostic impact of concomitant mutations in KRAS and TP53 or STK11. Lung Cancer 2019;130:50-8.
31. Djureinovic D, Hallström BM, Horie M, et al. Profiling cancer testis antigens in non-small-cell lung cancer. JCI Insight 2016;1:e86837.
32. Micke P, Edlund K, Holmberg L, et al. Gene copy number aberrations are associated with survival in histologic subgroups of non-small cell lung cancer. J Thorac Oncol 2011;6:1833-40.
33. Botling J, Edlund K, Lohr M, et al. Biomarker discovery in non-small cell lung cancer: integrating gene expression profiling, meta-analysis, and tissue microarray validation. Clin Cancer Res 2013;19:194-204.
34. Lira ME, Choi YL, Lim SM, et al. A single-tube

multiplexed assay for detecting ALK, ROS1, and RET fusions in lung cancer. J Mol Diagn 2014;16:229-43.
35. Haas BJ, Dobin A, Li B, et al. Accuracy assessment of fusion transcript detection via read-mapping and de novo fusion transcript assembly-based methods. Genome Biol 2019;20:213.
36. Schoonjans F. MedCalc's Diagnostic test evaluation calculator [Internet]. MedCalc. [cited 2022 Aug 5]. Available online: https://www.medcalc.org/calc/diagnostic_test.php
37. Yoshida A, Tsuta K, Wakai S, et al. Immunohistochemical detection of ROS1 is useful for identifying ROS1 rearrangements in lung cancers. Mod Pathol 2014;27:711-20.
38. Zhang Q, Wu C, Ding W, et al. Prevalence of ROS1 fusion in Chinese patients with non-small cell lung cancer. Thorac Cancer 2019;10:47-53.
39. Fu S, Liang Y, Lin YB, et al. The Frequency and Clinical Implication of ROS1 and RET Rearrangements in Resected Stage IIIA-N2 Non-Small Cell Lung Cancer Patients. PLoS One 2015;10:e0124354.
40. Wu J, Lin Y, He X, et al. Comparison of detection methods and follow-up study on the tyrosine kinase inhibitors therapy in non-small cell lung cancer patients with ROS1 fusion rearrangement. BMC Cancer 2016;16:599.
41. Davies KD, Le AT, Theodoro MF, et al. Identifying and targeting ROS1 gene fusions in non-small cell lung cancer. Clin Cancer Res 2012;18:4570-9.
42. Zhao W, Choi YL, Song JY, et al. ALK, ROS1 and RET rearrangements in lung squamous cell carcinoma are very rare. Lung Cancer 2016;94:22-7.
43. Zhu Q, Zhan P, Zhang X, et al. Clinicopathologic characteristics of patients with ROS1 fusion gene in non-small cell lung cancer: a meta-analysis. Transl Lung Cancer Res 2015;4:300-9.
44. Mansour MSI, Malmros K, Mager U, et al. PD-L1 Expression in Non-Small Cell Lung Cancer Specimens: Association with Clinicopathological Factors and Molecular Alterations. Int J Mol Sci 2022;23:4517.
45. Zacharias M, Absenger G, Kashofer K, et al. Reflex testing in non-small cell lung carcinoma using DNA- and RNA-based next-generation sequencing—a single-center experience. Transl Lung Cancer Res 2021;10:4221-34.
46. Mattsson JS, Brunnström H, Jabs V, et al. Inconsistent results in the analysis of ALK rearrangements in non-small cell lung cancer. BMC Cancer 2016;16:603.
47. Elfving H, Broström E, Moens LNJ, et al. Evaluation of NTRK immunohistochemistry as a screening method for NTRK gene fusion detection in non-small cell lung cancer. Lung Cancer 2021;151:53-9.
48. Shaw AT, Ou SH, Bang YJ, et al. Crizotinib in ROS1-rearranged non-small-cell lung cancer. N Engl J Med 2014;371:1963-71.
49. Davies KD, Le AT, Sheren J, et al. Comparison of Molecular Testing Modalities for Detection of ROS1 Rearrangements in a Cohort of Positive Patient Samples. J Thorac Oncol 2018;13:1474-82.
50. Camidge DR, Kono SA, Flacco A, et al. Optimizing the detection of lung cancer patients harboring anaplastic lymphoma kinase (ALK) gene rearrangements potentially suitable for ALK inhibitor treatment. Clin Cancer Res 2010;16:5581-90.
51. Huang RSP, Smith D, Le CH, et al. Correlation of ROS1 Immunohistochemistry With ROS1 Fusion Status Determined by Fluorescence In Situ Hybridization. Arch Pathol Lab Med 2020;144:735-41.
52. Hanlon Newell A, Liu W, Bubendorf L, et al. MA26.07 ROS1 (SP384) Immunohistochemistry Inter-Reader Precision Between 12 Pathologists. J Thorac Oncol 2018;13:S452-3.
53. Conde E, Hernandez S, Benito A, et al. Screening for ROS1 fusions in patients with advanced non-small cell lung carcinomas using the VENTANA ROS1 (SP384) Rabbit Monoclonal Primary Antibody. Expert Rev Mol Diagn 2021;21:437-44.
54. Acquaviva J, Wong R, Charest A. The multifaceted roles of the receptor tyrosine kinase ROS in development and cancer. Biochim Biophys Acta 2009;1795:37-52.
55. Mescam-Mancini L, Lantuéjoul S, Moro-Sibilot D, et al. On the relevance of a testing algorithm for the detection of ROS1-rearranged lung adenocarcinomas. Lung Cancer 2014;83:168-73.
56. Wilcock DM, Schmidt RL, Furtado LV, et al. Histologic and Molecular Characterization of Non-Small Cell Lung Carcinoma With Discordant ROS1 Immunohistochemistry and Fluorescence In Situ Hybridization. Appl Immunohistochem Mol Morphol 2022;30:19-26.
57. Zhao J, Chen X, Zheng J, et al. A genomic and clinicopathological study of non-small-cell lung cancers with discordant ROS1 gene status by fluorescence in-situ hybridisation and immunohistochemical analysis. Histopathology 2018;73:19-28.
58. Mino-Kenudson M. Immunohistochemistry for predictive biomarkers in non-small cell lung cancer. Transl Lung Cancer Res 2017;6:570-87.
59. Lee SE, Lee B, Hong M, et al. Comprehensive analysis of

RET and ROS1 rearrangement in lung adenocarcinoma. Mod Pathol 2015;28:468-79.
60. Gregg JP, Li T, Yoneda KY. Molecular testing strategies in non-small cell lung cancer: optimizing the diagnostic journey. Transl Lung Cancer Res 2019;8:286-301.
61. Elfving H, Mattsson JSM, Lindskog C, et al. Programmed Cell Death Ligand 1 Immunohistochemistry: A Concordance Study Between Surgical Specimen, Biopsy, and Tissue Microarray. Clin Lung Cancer 2019;20:258-262.e1.

Cite this article as: Thurfjell V, Micke P, Yu H, Krupar R, Svensson MA, Brunnström H, Lamberg K, Moens LNJ, Strell C, Gulyas M, Helenius G, Yoshida A, Goldmann T, Mattsson JSM. Comparison of ROS1-rearrangement detection methods in a cohort of surgically resected non-small cell lung carcinomas. Transl Lung Cancer Res 2022;11(12):2477-2494. doi: 10.21037/tlcr-22-504

Supplementary

Table S1 Patient characteristics of NSCLC patients in the Uppsala I cohort (surgically resected between 1995–2005)

Characteristics	Uppsala I				
	Affymerix Gene expression, n (%)	FISH, n (%)	Clone D4D6, n (%)	Clone SP384, n (%)	Clone EPMGHR2, n (%)
All cases	187 (100.0)	313 (100.0)	342 (100.0)	333 (100.0)	302 (100.0)
Sex					
Male	101 (54.0)	166 (53)	181 (52.9)	177 (53.2)	164 (54.3)
Female	86 (46.0)	147 (47)	161 (47.1)	156 (46.8)	138 (45.7)
Age at diagnosis					
≤70 years	145 (77.5)	218 (69.6)	236 (69.0)	230 (69.1)	210 (69.5)
>70 years	42 (22.5)	95 (30.4)	106 (31.0)	103 (30.9)	92 (30.5)
Smoking history					
Current smoker	94 (50.3)	150 (47.9)	159 (46.5)	156 (46.8)	142 (47.0)
Former smoker	79 (42.2)	136 (43.5)	149 (43.6)	146 (43.8)	132 (43.7)
Never smoker	14 (7.5)	25 (8.0)	32 (9.4)	29 (8.7)	26 (8.6)
Missing	0 (0)	2 (0.6)	2 (0.6)	2 (0.6)	2 (0.6)
TNM-stage at diagnosis (8th edition)					
IA1	1 (0.5)	1 (0.3)	1 (0.3)	1 (0.3)	1 (0.3)
IA2	12 (6.4)	26 (8.3)	27 (7.9)	25 (7.5)	25 (8.3)
IA3	23 (12.3)	45 (14.4)	49 (14.3)	49 (14.7)	42 (13.9)
IB	27 (14.4)	52 (16.6)	57 (16.7)	57 (17.1)	54 (17.9)
IIA	16 (8.6)	20 (6.4)	23 (6.7)	20 (6.0)	18 (6.0)
IIB	57 (30.5)	84 (26.8)	92 (26.9)	91 (27.3)	80 (26.5)
IIIA	38 (20.3)	68 (21.7)	73 (21.3)	71 (21.3)	66 (21.9)
IIIB	11 (5.9)	12 (3.8)	16 (4.7)	15 (4.5)	13 (4.3)
IIIC	0 (0)	0 (0)	0 (0)	0 (0)	0 (0)
IVA	0 (0)	0 (0)	0 (0)	0 (0)	0 (0)
IVB	2 (1.1)	5 (1.6)	4 (1.2)	4 (1.2)	3 (1.0)
Histology					
Adenocarcinoma	101 (54.0)	169 (54.0)	190 (55.6)	182 (54.7)	165 (54.6)
Squamous cell carcinoma	62 (33.2)	109 (34.8)	115 (33.6)	114 (34.2)	107 (35.4)
Large cell carcinoma	24 (12.8)	35 (11.2)	37 (10.8)	37 (11.1)	30 (9.9)
WHO performance status					
0	100 (53.5)	163 (52.1)	180 (52.6)	175 (52.6)	160 (53)
1	71 (38.0)	120 (38.3)	129 (37.7)	126 (37.8)	113 (37.4)
2	12 (6.4)	24 (7.7)	27 (7.9)	26 (7.8)	24 (7.9)
3	4 (2.1)	5 (1.6)	5 (1.5)	5 (1.5)	4 (1.3)
4	0 (0.0)	1 (0.3)	1 (0.3)	1 (0.3)	1 (0.3)
Mean follow-up (months)	61.3	61.9	61.6	60.7	61.5

NSCLC, non-small cell lung cancer; TNM, tumor (T), nodes (N), and metastases (M); FISH, fluorescence in situ hybridization.

https://dx.doi.org/10.21037/tlcr-22-504

Table S2 Patient characteristics of NSCLC patients in the Uppsala II cohort (surgically resected between 2006-2010).

Characteristics	Uppsala II				
	RNAseq Gene expression, n (%)	FISH, n (%)	Clone D4D6, n (%)	Clone SP384, n (%)	Clone EPMGHR2, n (%)
All cases	182 (100.0)	317 (100.0)	323 (100.0)	306 (100.0)	291 (100.0)
Sex					
Male	88 (48.4)	159 (50.2)	161 (49.8)	155 (50.7)	144 (49.5)
Female	94 (51.6)	158 (49.8)	162 (50.2)	151 (49.3)	147 (50.5)
Age at diagnosis					
≤70 years	107 (58.8)	203 (64.0)	207 (64.1)	194 (63.4)	186 (63.9)
>70 years	75 (41.2)	114 (36.0)	116 (35.9)	112 (36.6)	105 (36.1)
Smoking History					
Current smoker	87 (47.8)	164 (51.7)	165 (51.1)	156 (51.0)	152 (52.2)
Former smoker	78 (42.9)	119 (37.5)	123 (38.1)	117 (38.2)	106 (36.4)
Never smoker	17 (9.3)	34 (10.7)	35 (10.8)	33 (10.8)	33 (11.3)
Missing	0 (0)	0 (0)	0 (0)	0 (0)	0 (0)
TNM-stage at diagnosis (8th edition)					
IA1	0 (0.0)	12 (3.8)	12 (3.7)	11 (3.6)	10 (3.4)
IA2	38 (20.9)	67 (21.1)	69 (21.4)	64 (20.9)	60 (20.6)
IA3	35 (19.2)	75 (23.7)	75 (23.2)	70 (22.9)	68 (23.4)
IB	22 (12.1)	33 (10.4)	34 (10.5)	34 (11.1)	33 (11.3)
IIA	14 (7.7)	20 (6.3)	20 (6.2)	20 (6.5)	20 (6.9)
IIB	30 (16.5)	45 (14.2)	45 (13.9)	43 (14.1)	39 (13.4)
IIIA	37 (20.3)	50 (15.8)	52 (16.1)	49 (16.0)	47 (16.2)
IIIB	6 (3.3)	11 (3.5)	11 (3.4)	10 (3.3)	9 (3.1)
IIIC	0 (0)	0 (0.0)	0 (0.0)	0 (0.0)	0 (0.0)
IVA	0 (0)	4 (1.3)	5 (1.5)	5 (1.6)	5 (1.7)
IVB	0 (0)	0 (0)	0 (0)	0 (0)	0 (0)
Histology					
Adenocarcinoma	108 (59.3)	200 (63.1)	206 (63.8)	192 (62.7)	180 (61.9)
Squamous cell carcinoma	61 (33.5)	96 (30.3)	96 (29.7)	93 (30.4)	90 (30.9)
Large cell carcinoma	4 (2.2)	5 (1.6)	5 (1.5)	5 (1.6)	5 (1.7)
Adenosquamous carcinoma	3 (1.6)	5 (1.6)	5 (1.5)	5 (1.6)	5 (1.7)
Sarcomatoid carcinoma	1 (0.5)	2 (0.6)	2 (0.6)	2 (0.7)	2 (0.7)
Large cell neuroendocrine carcinoma	5 (2.7)	9 (2.8)	9 (2.8)	9 (2.9)	9 (3.1)
WHO performance status					
0	114 (62.6)	198 (62.5)	202 (62.5)	192 (62.7)	182 (62.5)
1	66 (36.3)	116 (36.6)	118 (36.5)	111 (36.3)	106 (36.4)
2	2 (1.1)	3 (0.9)	3 (0.9)	3 (1.0)	3 (1.0)
3	0 (0)	0 (0)	0 (0)	0 (0)	0 (0)
4	0 (0.0)	0 (0)	0 (0)	0 (0)	0 (0.0)
Mean follow-up (months)	72.2	70	70.1	70.3	70

NSCLC, non-small cell lung cancer; TNM, tumor (T), nodes (N), and metastases (M); FISH, fluorescence in situ hybridization.

https://dx.doi.org/10.21037/tlcr-22-504

Table S3 Targeted NanoString digital counting was performed using a custom-designed fusion gene assay, based on Lira et al. (2014), with additional probes for ROS proto-oncogene 1 (ROS1)

Assay type	Probe name	Accession	Position	Target sequence
3’/5’	ROS1_5’-1	NM_002944.2	501-600	TACCAACTGCTCCCTTTGCTTCTTCCATTGGAAGCCAC AATATGACATTACGATGGAAATCTGCAAACTTCTCTGGA GTAAAATACATCATTCAGTGGAA
3’/5’	ROS1_5’-2	NM_002944.2	2917-3016	TCAAGAAATAGGTCAGAAAACCAGTGTCTCTGTTTTGG AACCAGCCAGATTTAATCAGTTCACAATTATTCAGACATC CCTTAAGCCCCTGCCAGGGAAC
3’/5’	ROS1_5’-3	NM_002944.2	3907-4006	GCACCTCTACTTTGCACTGAAAGAATCACAAAATGGAAT GCAAGTATTTGATGTTGATCTTGAACACAAGGTGAAATAT CCCAGAGAGGTGAAGATTCAC
3’/5’	ROS1_5’-4	NM_002944.2	5019-5118	CTCTAAGACAAAGTGAATTTCCAAATGGAAGGCTCACT CTCCTTGTTACTAGACTGTCTGGTGGAAATATTTATGTGT TAAAGGTTCTTGCCTGCCACTC
3’/5’	ROS1_3’-1	NM_002944.2	6166-6265	GGAGAAGATTGAATTCCTGAAGGAGGCACATCTGATGA GCAAATTTAATCATCCCAACATTCTGAAGCAGCTTGGAG TTTGTCTGCTGAATGAACCCCAA
3’/5’	ROS1_3’-2	NM_002944.2	6363-6462	ACCTTGTAGACCTGTGTGTAGATATTTCAAAAGGCTGTG TCTACTTGGAACGGATGCATTTCATTCACAGGGATCTGG CAGCTAGAAATTGCCTTGTTTC
3’/5’	ROS1_3’-3	NM_002944.2	6750-6849	GAAATTGTCCTGATGATCTGTGGAATTTAATGACCCAGT GCTGGGCTCAAGAACCCGACCAAAGACCTACTTTTCAT AGAATTCAGGACCAACTTCAGTT
3’/5’	ROS1_3’-4	NM_002944.2	7262-7361	AGAGAGTTGAGATAAACACTCTCATTCAGTAGTTACTGA AAGAAAACTCTGCTAGAATGATAAATGTCATGGTGGTCT ATAACTCCAAATAAACAATGCA
Specific fusion	SLC34A2-ROS1_ S4:R32	-	SLC34A2-ROS1_ S4:R32	TTTCGTGTGCTCCCTGGATATTCTTAGTAGCGCCTTCCA GCTGGTTGGAGCTGGAGTCCCAAATAAACCAGGCATTC CCAAATTACTAGAAGGGAGTAAA
Specific fusion	CD74-ROS1_C6:R32	-	CD74-ROS1_C6:R32	AATGAGCAGGCACTCCTTGGAGCAAAAGCCCACTGAC GCTCCACCGAAAGCTGGAGTCCCAAATAAACCAGGCA TTCCCAAATTACTAGAAGGGAGTAAA
Specific fusion	SDC4-ROS1_S2:R32	-	SDC4-ROS1_S2:R32	GCCCGGGCAGGAATCTGATGACTTTGAGCTGTCTGGC TCTGGAGATCTGGCTGGAGTCCCAAATAAACCAGGCAT TCCCAAATTACTAGAAGGGAGTAAA
Specific fusion	SLC34A2-ROS1_ S13del2046:R32	-	SLC34A2-ROS1_ S13del2046:R32	CAAGGCTCCTGAGACCTTTGATAACATAACCATTAGCAG AGAGGCTCAGGCTGGAGTCCCAAATAAACCAGGCATT CCCAAATTACTAGAAGGGAGTAAA
Specific fusion	SLC34A2-ROS1_ S4:R34	-	SLC34A2-ROS1_ S4:R34	TTTCGTGTGCTCCCTGGATATTCTTAGTAGCGCCTTCCA GCTGGTTGGAGATGATTTTTGGATACCAGAAACAAGTTT CATACTTACTATTATAGTTGGA
Specific fusion	EZR-ROS1_E10:R34	-	EZR-ROS1_E10:R34	GATGCTGCGGCTGCAGGACTATGAGGAGAAGACAAAG AAGGCAGAGAGAGATGATTTTTGGATACCAGAAACAAG TTTCATACTTACTATTATAGTTGGA
Specific fusion	SDC4-ROS1_S4:R34	-	SDC4-ROS1_S4:R34	CAGCACTGTGCAGGGCAGCAACATCTTTGAGAGAACG GAGGTCCTGGCAGATGATTTTTGGATACCAGAAACAAG TTTCATACTTACTATTATAGTTGGA
Specific fusion	GOPC-ROS1_ G8:R35	-	GOPC-ROS1_G8:R35	CCCTGGTGCTAGTTGCAAAGACACAAGTGGGGAAATC AAAGTATTACAAGTCTGGCATAGAAGATTAAAGAATCAAA AAAGTGCCAAGGAAGGGGTGACA
Specific fusion	TPM3-ROS1_T8:R35	-	TPM3-ROS1_T8:R35	TGCTGAGAGATCGGTAGCCAAGCTGGAAAAGACAATTG ATGACCTGGAAGTCTGGCATAGAAGATTAAAGAATCAAA AAAGTGCCAAGGAAGGGGTGACA
Specific fusion	LRIG3-ROS1_ L16:R35	-	LRIG3-ROS1_L16:R35	TGTCACATCTTCAGGTGCTGGATTTTTCTTACCACAACA TGACAGTAGTGTCTGGCATAGAAGATTAAAGAATCAAAA AAGTGCCAAGGAAGGGGTGACA
Specific fusion	GOPC-ROS1_ G4:R36	-	GOPC-ROS1_G4:R36	TATGGGGCGAGACTAGCTGCCAAGTACTTGGATAAGGA ACTGGCAGGAAGTACTCTTCCAACCCAAGAGGAGATT GAAAATCTTCCTGCCTTCCCTCGGG
Specific fusion	GOPC-ROS1_ G7:R35	-	GOPC-ROS1_G7:R35	TATATGGGGCGAGACTAGCTGCCAAGTACTTGGATAAG GAACTGGCAGGATCTGGCATAGAAGATTAAAGAATCAAA AAAGTGCCAAGGAAGGGGTGACA
Specific fusion	LRIG3-ROS1 _ L16:R35	-	LRIG3-ROS1 _L16:R35	TTTGTCACATCTTCAGGTGCTGGATTTTTCTTACCACAA CATGACAGTAGTCTGGCATAGAAGATTAAAGAATCAAAA AAGTGCCAAGGAAGGGGTGACA

https://dx.doi.org/10.21037/tlcr-22-504